Magnetic properties of amorphous iron

Mark W. Grinstaff
Department of Chemistry and the Materials Research Laboratory, University of Illinois at Urbana-Champaign, 505 South Mathews, Urbana, Illinois 61801

Myron B. Salamon
Department of Physics and the Materials Research Laboratory, University of Illinois at Urbana-Champaign, 1110 West Green Street, Urbana, Illinois 61801-3080

Kenneth S. Suslick
Department of Chemistry and the Materials Research Laboratory, University of Illinois at Urbana-Champaign, 505 South Mathews, Urbana, Illinois 61801

(Received 6 July 1992; revised manuscript received 11 February 1993)

Ultrasonic irradiation of iron pentacarbonyl was shown recently to result in the formation of fine ($\simeq 30$ nm) amorphous, elemental-iron particles. We have measured the magnetic properties of an aggregate of these particles and find that they are soft ferromagnets with a Curie temperature in excess of 580 K. The exchange stiffness, as manifested through the coefficient of the $T^{3/2}$ temperature dependence in Bloch's law, is 30% of that of crystalline Fe. The low-temperature magnetization curves approach saturation as the inverse square root of applied field, which is characteristic of systems with random anisotropy fields. We argue that the results are consistent with the properties of an aggregate of amorphous Fe particles of nonspherical shape, giving rise to local shape anisotropy.

I. INTRODUCTION

Amorphous metallic alloys ("metallic glasses") lack long-range crystalline order and are similar to frozen liquids. They are structurally distinct from their crystalline counterparts and have different physical properties.[1-3] The magnetic properties, in particular, have been studied extensively,[4] especially those of iron-based materials because of their potential technological applications. With few exceptions,[4-6] Fe-based metallic glasses involve eutectic alloys such as Fe alloyed with B, P, and C. The crystallization temperature of amorphous Fe has been predicted to be on the order of 800 K;[4] once synthesized, it should be stable at ordinary temperatures.

We have recently prepared amorphous *elemental*-iron powder by the ultrasonic irradiation of iron pentacarbonyl and demonstrated its amorphous nature by x-ray powder diffraction, transmission electron microscopy (TEM) microdiffraction, differential scanning calorimetry, and scanning electron microscopy.[7] Transmission electron micrographs of the amorphous iron before and after crystallization are shown in Fig. 1. The amorphous powder is an agglomerate of small iron particles with diameters ≤ 30 nm. TEM microdiffraction of the amorphous iron shows only a diffuse ring, which is characteristic of amorphous materials [Fig. 1(a), inset]. Prolonged exposure of the amorphous iron to the electron beam induces crystallization and the diffraction rings of α-iron become prevalent [Fig. 1(b), inset].

Synthesis of the amorphous iron is carried out using the extreme reaction conditions generated by acoustic cavitation, i.e., the formation, growth, and implosive collapse of bubbles during ultrasonic irradiation;[8] high temperatures and pressures are generated by the implosion. Using comparative rate thermometry we have measured the temperature reached during bubble collapse to be ≈ 5000 K,[9] and recent sonoluminescence experiments have confirmed a comparable effective emission temperature.[10] Single-bubble sonoluminescence experiments suggest that the emission lifetime is < 1 ns.[11] Consequently, the heating and cooling rates during cavitational collapse are extremely fast ($> 10^9$ K/s). The extremely rapid cavitational cooling rate is orders of magnitude faster than is possible using techniques such as splat cooling, roller quenching, or quench condensing. The quenching rate required to produce amorphous iron has been predicted to be 10^{10} K/s,[12] and this rate is apparently achieved using this sonochemical technique.

II. EXPERIMENT

Ultrasonic irradiation of iron pentacarbonyl, $Fe(CO)_5$, yields a dull black powder.[5] The application of ultrasound to chemical synthesis[6,13] and the experimental apparatus are described in detail elsewhere.[14] Pure $Fe(CO)_5$ or $4.0M$ solutions in decane were irradiated at 0 °C with a high-intensity ultrasonic horn (Sonics and Materials, model VC-600, 0.5 in. Ti horn, 20 KHz, ≈ 80 W/cm^2) for 3 h under argon. After irradiation, the iron powder produced was collected by filtration and washed with dry pentane in an inert atmosphere box (Vacuum Atmospheres, < 1 ppm O_2). The noncrystalline structure of the iron powder was confirmed using a variety of physical techniques including TEM microdiffraction, x-ray powder diffraction, and differential scanning calorimetry (DSC).[7] The DSC profile, for example, shows an exothermic peak at ≈ 585 K corresponding to crystallization of the amorphous iron. X-ray powder diffraction showed

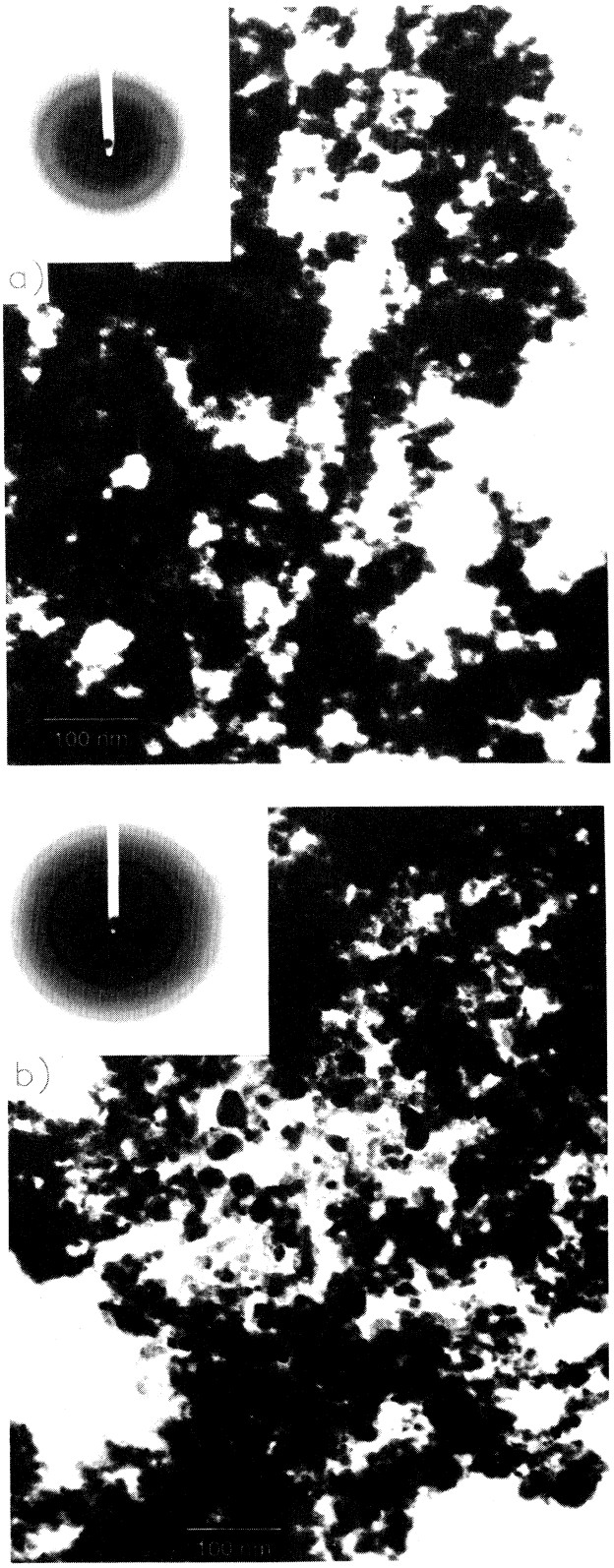

FIG. 1. Transmission electron micrographs and microdiffraction patterns of amorphous iron before (a) and after crystallization (b) (Phillips EM400T). The insets show the corresponding diffraction patterns.

that the amorphous iron crystallizes exclusively to α-iron. Bulk elemental analysis determined the iron powder to be >96-wt % iron with a trace amount of carbon (<3 wt %) and oxygen (1 wt %). The carbon most likely originates from the decomposition of pentane (used to wash the reactive iron powder after synthesis) and from small amounts of remnant CO.

Magnetic data were recorded using a Quantum Design MPMS SQUID magnetometer. Iron samples were prepared for magnetic measurements in an inert atmosphere box. Gelatin capsules were filled with a known amount of iron powder and then packed with quartz wool. The capsule was then double bottled and transferred to the SQUID magnetometer sample chamber. Curie point determinations were done with a Perkin-Elmer TGA7 thermally controlled microbalance in a magnetic field. The iron powder was loaded into an aluminum capsule in the inert atmosphere box, double bottled, and transferred to the TGA. A local magnetic field was induced around the iron sample in the TGA by a small permanent magnet.

III. RESULTS AND DISCUSSION

The sonochemically synthesized amorphous iron powder is a soft ferromagnetic material as shown by hysteresis loops taken at 300 and 5 K and plotted in Fig. 2. The material is significantly more difficult to magnetize at 5 K, at which temperature there is a small coercive field, $H_c \simeq 190$ Oe. However, the remanant magnetization at 5 K decays very rapidly (93% reduction 5 min after reducing the field to zero), and this suggests that H_c may be an artifact of the speed at which the hysteresis loop data were taken (approximately 2 min per datum).

Even at relatively large applied fields, the magnetization first increases slightly with increasing temperature before decreasing normally. This is shown in Fig. 3, where the magnetization at an applied field of 20 kOe is plotted versus $T^{3/2}$. The amorphous Fe data above 50 K clearly follow Bloch's law,[15]

$$1-M_a(T)/M_a(0)=B_a T^{3/2} , \quad (1)$$

with $B_a=2.2\times10^{-5}$ K$^{-3/2}$ and $M_a(0)=156$ emu/g. The corresponding values for crystalline Fe are $B_c=3.5\times10^{-6}$ K$^{-3/2}$ and $M_c(0)=217$ emu/g. While the small particle size produces a long-wavelength cutoff in the spin-wave spectrum, its effect should become important only well below 1 K. Assuming that every Fe atom contributes equally to $M_a(0)$, we find the effective Fe moment to be $\mu_a=1.6\mu_B$ in the amorphous state, compared with the crystalline value $\mu_c=2.2\mu_B$. However, the magnetization is not saturated at 20 kOe, an issue we return to below. The larger value of B reflects both the smaller effective moment and a reduced effective exchange constant in the amorphous material, and consequently a smaller T_C. In Fig. 4, we show the result of force measurements on sonicated and crystalline Fe powders. The amorphous powder exhibits a transition at 583 K (310 °C), followed by higher-temperature transitions associated with crystalline iron. Because crystalli-

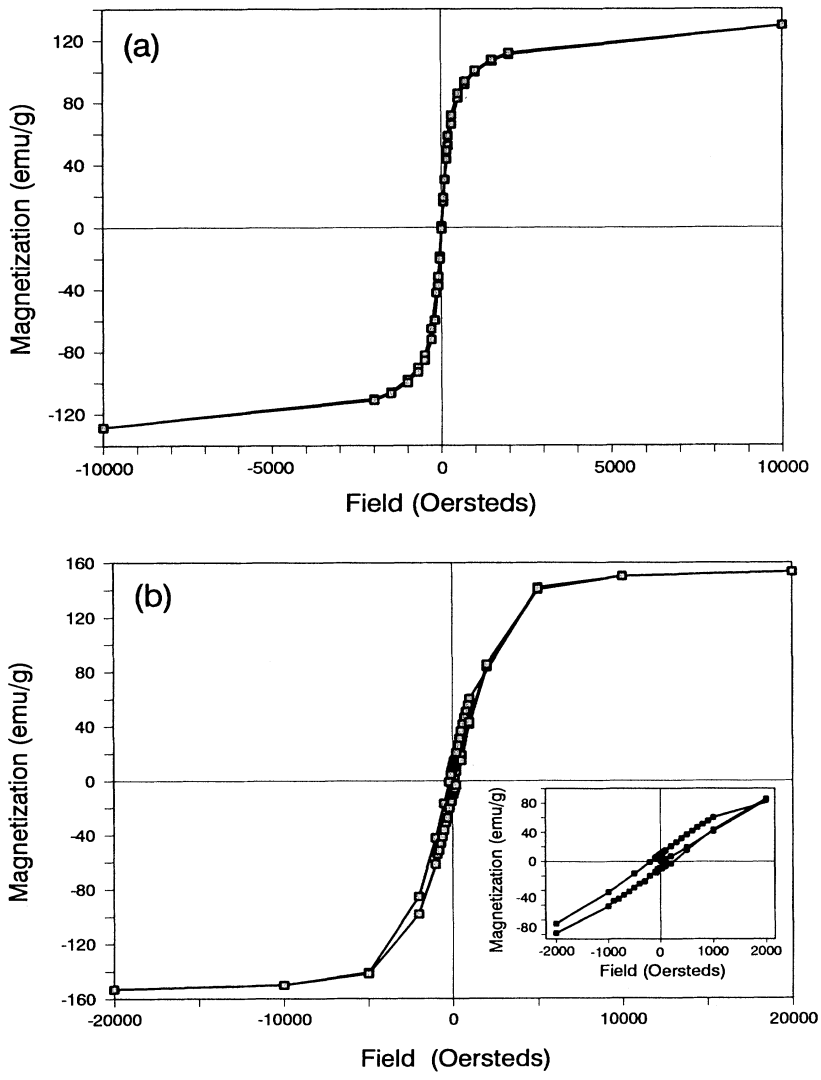

FIG. 2. Hysteresis loops for amorphous Fe (a) at 300 K and (b) at 5 K. The coercive field at 5 K depends on the time scale of the measurement.

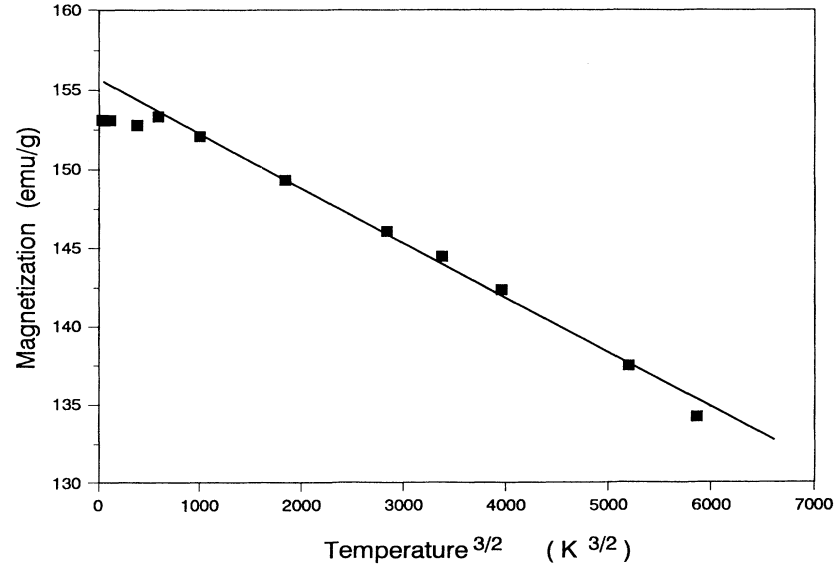

FIG. 3. Magnetization measured in a field of 20 kOe vs the $\frac{3}{2}$ power of temperature. The line is a fit to Bloch's law. Note the slight maximum near 50 K.

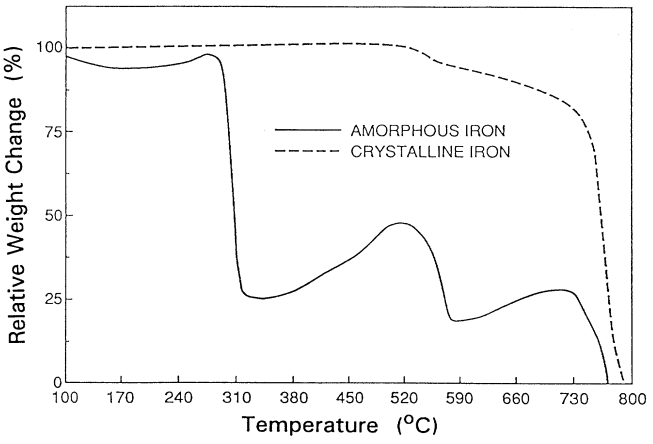

FIG. 4. Curie point determination for amorphous (solid curve) and crystalline iron (dashed curve). Data obtained on a Perkin-Elmer TGA7.

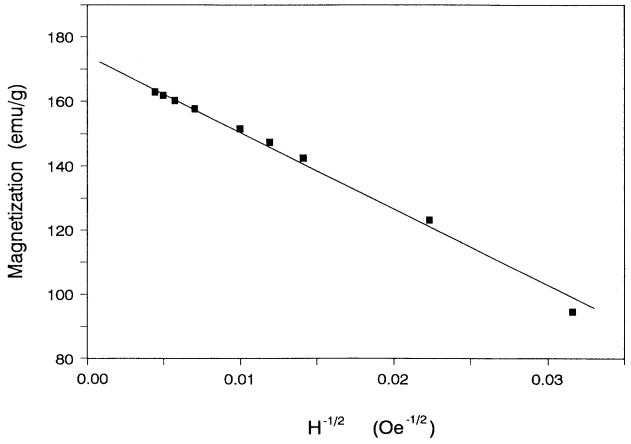

FIG. 5. Magnetization vs $H^{-1/2}$ for amorphous iron. The solid line is a fit to correlated-spin-glass theory [17].

zation of the amorphous iron occurs at 585 K (312 °C), this temperature places a lower limit on T_C for amorphous iron. The feature near 848 K (575 °C) in both amorphous and crystalline Fe is very likely the Curie point of Fe_3O_4; unsurprisingly, it appears that some oxidation occurs during the thermogravimetric analysis.

The reduced moment per Fe atom and the low-temperature decrease in magnetization could be attributed to superparamagnetism.[16] However, magnetization data taken at different temperatures are not superimposable when plotted versus H/T, as required for superparamagnetic behavior. It is unlikely, therefore, that the maximum observed $M(H,T)$ curves for $H \leq 20$ kOe is the result of Néel blocking. Neither is there evidence for spin-glass behavior. The results are also quite different from those obtained on fine iron particles produced by nanocrystalline methods.[17]

A possible source of the decrease in low-field magnetization at low temperatures is the presence of random anisotropy, either from random local crystal fields or random shape anisotropy. The phenomenology of such systems, which are not true ferromagnets but rather "correlated spin glasses," has been treated in detail by Chudnovsky and co-workers.[18] This approach has been employed in the study of other amorphous materials such as $Gd_{72}Fe_{10}Ga_{18}$,[19] $Fe_7Ni_{73}P_{14}B_6$,[20] and $Mn_{48}B_{56}$.[21] A characteristic of such systems is the gradual approach to saturation which, at moderate fields satisfies

$$1-M_a(H,T)/M_a(\infty,T)=\tfrac{1}{15}(H_s/H)^{1/2} . \quad (2)$$

The field H_s can be written as $H_s=H_r^4/H_e^3$, where $H_r M_a(T)/2$ is a measure of the random anisotropy energy and $H_e M_a(T)$ measures the energy cost to rotate the direction of magnetization by 90° in the distance R_s over which the anisotropy direction rotates by the same amount. H_e is proportional to the exchange stiffness constant, and decreases as the inverse square of R_s. Figure 5 is a plot of the magnetization at 5 K versus $H^{-1/2}$. The approach to saturation follows Eq. (3) extremely well over the range $3 \leq H \leq 50$ kOe. The true saturation moment is $\mu_a=173$ emu/g and $H_s=34$ kOe; the former value corresponds to a moment of $1.7\mu_B$ per Fe atom, which we will use in the discussion that follows. This value agrees well with that obtained by extrapolating the Fe moment in Fe-B glasses to the pure, amorphous iron limit.[22]

The standard mean-field expressions for the transition temperature lead to the prediction

$$T_C^a=T_C^c\left[\frac{z_a}{z_c}\right]\left[\frac{B_c S_c}{B_a S_a}\right]^{2/3}\left[\frac{S_a+1}{S_c+1}\right], \quad (3)$$

where z_a and z_c are the coordination numbers and $S_{a,c}=\mu_{a,c}/2\mu_B$, effective spins of the amorphous and crystalline materials. If we assume that the amorphous phase is locally close packed, we have $z_a/z_c \simeq 1.5$, which leads to a predicted Curie temperature $T_C^a=480$ K, reasonably close to the observed $T_C^a \geq 580$ K. The spin factors are relatively unimportant; the primary effect is the change in the effective exchange interaction as reflected in B_a.

In order to discuss the source of the random anisotropy, we first need to determine H_e, which we do using mean-field expressions. The same values of B_a and S_a lead to the estimate $H_e \simeq 6.4\times10^5(a/R_s)^2$ Oe, where a is the average Fe-Fe spacing, assumed to be the same for amorphous and crystalline iron. The resulting random anisotropy field is $H_r \simeq 310(a/R_s)^{3/2}$ kOe. The largest source of randomness arises from the distribution of particle shapes which produce a random demagnetizing field, whose scale is set by the magnetization, approximately 1 kOe. For this to be the source of H_r requires that $R_s/a \simeq 46$, which is roughly the size of the amorphous Fe particles. The cubic anisotropy field of bcc iron is also on the order of 1 kOe, but for this to be the source of H_r requires a crystalline coherence over long distances which is inconsistent with the amorphous nature of this material.

Ferromagnetic resonance measurements were also made at 9 GHz on the amorphous iron powder. An extremely broad resonance was observed, approximately 5-kOe peak-to-peak separation in the derivative signal at 140 K. The width increases with decreasing temperature. These observations are consistent with a distribution of particle shapes which can spread the field required for resonance over a range of order $4\pi M_a(T) \simeq 12$ kOe.

IV. CONCLUSIONS

In summary, the amorphous iron synthesized from sonolysis of iron pentacarbonyl has been shown to be a soft ferromagnet with a saturation magnetization of ≈ 173 emu/g. The amorphous iron has an effective moment of $\mu_a = 1.7\mu_B$. The magnetization follows Bloch's $T^{2/3}$ law, from which we deduce that the effective exchange constant is only 30% that of crystalline Fe. However, the Curie temperature exceeds 580 K. There have been numerous estimates of the Curie temperature of amorphous Fe obtained by extrapolating to 100% Fe concentration. The results are strongly system dependent: Fe–rare-earth systems[23] (270 K), melt spun Fe (Ref. 24) (≈ 400 K), Fe-metalloid (Ref. 25) (≈ 320 K), and Fe-Zr (≈ 100 K). This wide variation suggests that such extrapolations are unreliable. The relatively high T_c^a results in part from the increased coordination number $z_a \simeq 12$ of a close-packed amorphous structure relative to $z_c = 8$ for a bcc crystal. The magnetic behavior of amorphous iron powder is not that of a superparamagnet nor of a single domain ferromagnet. Rather, the approach to saturation is consistent with the behavior of a "correlated spin glass," with randomness provided by a distribution of particle shapes.

ACKNOWLEDGMENTS

We gratefully acknowledge N. Tea for carrying out magnetic resonance measurements and the helpful discussions with Professor W. Saslow. The helpful discussions with Dr. A. C. Cichowlas and Dr. S.-B. Choe are also appreciated. This work was supported in part by NSF Grant No. DMR-8920538 through the Illinois Materials Research Laboratory and by financial support to M.W.G. by NSF Grant No. CHE-8915020.

[1]S. J. Takayama, Mater. Sci. **11**, 164 (1976).
[2]P. Haasen and R. I. Jaffee, *Amorphous Metals and Semiconductors* (Pergamon, London, 1986).
[3]*Processing of Structural Metals by Rapid Solidification,* edited by F. W. Froes and S. J. Savage (American Society for Metals, Metals Park, Ohio, 1987).
[4]T. Egami, Rep. Prog. Phys. **47**, 1601 (1984).
[5]J.-P. Lauriat, J. Non-Cryst. Solids **55**, 77 (1983).
[6]Y.-W. Kim, H.-M. Lin, and T. F. Kelly, Acta Metall. **37**, 247 (1989).
[7]K. S. Suslick, S. B. Choe, A. A. Cichowlas, and M. W. Grinstaff, Nature **353**, 414 (1991).
[8]K. S. Suslick, Science **247**, 1439 (1990); Sci. Am. **260**, 80 (1989).
[9]K. S. Suslick, R. E. Cline, Jr., and D. A. Hammerton, J. Am. Chem. Soc. **108**, 5641 (1986).
[10]E. B. Flint and K. S. Suslick, Science **253**, 1397 (1991).
[11]B. P. Barber and S. J. Putterman, Nature **352**, 318 (1991).
[12]H. S. Chen, Rep. Prog. Phys. **43**, 353 (1980).
[13]C. Einhorn, J. Einhorn, and J. L. Luche, Synthesis **11**, 787 (1989); J. Lindley and T. J. Mason, Chem. Soc. Rev. **16**, 275 (1987); K. S. Suslick, Adv. Organometal. Chem. **25**, 73 (1986).
[14]K. S. Suslick, J. W. Goodale, P. F. Schubert, and H. H. Wang, J. Am. Chem. Soc. **105**, 5781 (1983); K. S. Suslick and E. B. Flint, in *Experimental Organometallic Chemistry: A Practicum in Synthesis and Characterization,* edited by A. Wayda and M. Y. Darensbourg, (ACS Press, Washington, D.C., 1987), p. 195.
[15]C. Kittel, *Quantum Theory of Solids* (Wiley, New York, 1963), p. 56.
[16]C. P. Bean and I. S. Jacobs, J. Appl. Phys. **27**, 1448 (1956); J. L. Dormann, Rev. Phys. Appl. **16**, 275 (1981).
[17]S. U. Jen *et al.*, J. Mag. Magn. Mater. **96**, 82 (1991).
[18]E. M. Chudnovsky, J. Appl. Phys. **10**, 5770 (1988); E. M. Chudnovsky and R. A. Serota, Phys. Rev. B **26**, 2697 (1982); E.M. Chudnovsky, W. M. Saslow, and R. A. Serota, *ibid.* **33**, 251 (1986).
[19]D. J. Sellmymer and S. J. Nafis, Appl. Phys. **57**, 3584 (1985).
[20]M. J. Park, S. M. Bhagat, M. A. Manheimer, and K. Moorjani, Phys. Rev. B **33**, 2070 (1986).
[21]W. A. Bryden, T. S. Morgan, T. J. Kistenmacher, and K. Moorjani, J. Appl. Phys. **61**, 3661 (1987).
[22]N. Cowlam and G. E. Carr, J. Phys. F **15**, 1109 (1985).
[23]N. Heiman, K. Lee, and S. Kirkpatrick, J. Appl. Phys. **47**, 2634 (1976).
[24]K. Yano *et al.*, J. Magn. Mag. Mater. **104-107**, 131 (1992).
[25]T. Egami, Rep. Prog. Phys. **47**, 1601 (1984).

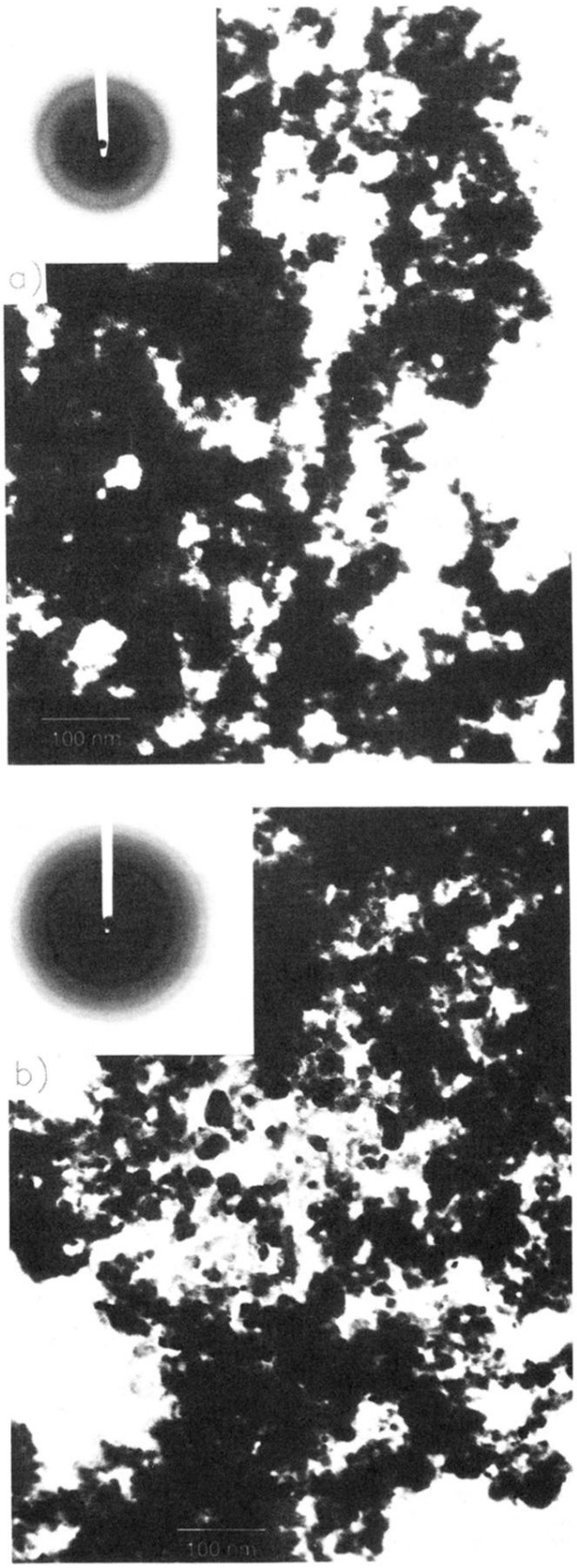

FIG. 1. Transmission electron micrographs and microdiffraction patterns of amorphous iron before (a) and after crystallization (b) (Phillips EM400T). The insets show the corresponding diffraction patterns.